Available online at www.sciencedirect.com
ScienceDirect
Dyes and Pigments 76 (2008) 236–242
DYES and PIGMENTS
www.elsevier.com/locate/dyepig

Synthesis, aggregation and photoconductive properties of alkoxycarbonyl substituted perylenes

Xiong Mo, Min-Min Shi, Jia-Chi Huang, Mang Wang, Hong-Zheng Chen*

Department of Polymer Science and Engineering, State Key Laboratory of Silicon Materials, Zhejiang University, Hangzhou 310027, PR China

Received 22 July 2006; received in revised form 20 August 2006; accepted 24 August 2006
Available online 16 October 2006

Abstract

A series of 3,4,9,10-tetra-(*n*-alkoxy-carbonyl)-perylene (PTAC, $n = 4, 6, 8, 10, 12$) derivatives with various alkyl chains were synthesized via a simple and efficient phase-transfer catalysis method. It was found that the length of the alkyl chains attached to the perylene skeleton greatly influenced aggregation behaviour. The finding that it was easier for PTAC derivatives with shorter alkyl chains to form crystal films was interpreted in terms of molecular volume and steric repulsion. The photoconductivity of the materials was investigated by xerographic photoinduced discharge technique and the results showed that photosensitivity increased with the decreasing length of the alkyl chain attached to perylene core. This result was consistent with the changing trend of aggregate structure observed for the PTAC derivatives used in this study: the shorter the substituted alkyl chain, the more ordered the film was and, thus, the greater was the photosensitivity.

Keywords: Perylene; Phase-transfer catalysis; Aggregate structure; Photoconductivity

1. Introduction

Electronic and opto-electronic devices based on organic semiconductors (which are usually organic dyes and pigments) offer an attractive alternative to conventional inorganic devices due to their potentially low costs, simple packaging and compatibility with flexible substrate. Thermal evaporation of organic semiconductors under vacuum typically yields thin films of the highest possible quality in terms of purity, grain size, and crystallinity. These evaporated films are useful for investigation of intrinsic transport and luminescence properties and in establishing upper performance thresholds. However, to fully realize the cost advantages associated with organic semiconductors, one would prefer to work with solution-based deposition process such as spin-coating and inkjet printing. Among the organic semiconductors that have been evaluated for practical applications, perylene derivatives are of great interest. Various perylene derivatives are promising materials for organic solar cells (OPVCs) [1–4], organic field-effect transistors (OFETs) [5,6], organic light emitting diodes (OLEDs) [7,8], etc. 3,4,9,10-Tetra-(*n*-alkoxy-carbonyl)-perylene (PTAC) compounds possess not only fluorescence characteristics similar to the parent compound perylene-3,4,9,10-tetracarboxylic dianhydride (PTCDA), but also display good solubility and the ability to form a liquid crystalline phase (LC) [9]. Due to the latter characteristic, they can form highly ordered films and may show super semiconductive performances. Unfortunately, the traditional esterification method of synthesizing PTAC is complicated and time-consuming (3–6 days) [10].

A considerable advantage of PTAC is its ability to form columnar liquid crystals, which are easy to expel defects in an annealing process [11]. This paper concerns an attempt to prepare PTAC derivatives of high purity and high yield via a simple phase-transfer catalysis (PTC) method [12]. A series of PTAC compounds with different substituents (i.e. alkyls having 4, 6, 8, 10 and 12 carbon atoms, respectively) were synthesized, and their molecular and electronic structures

* Corresponding author. Tel.: +86 571 8795 2557; fax: +86 571 8795 3733.
E-mail address: hzchen@zju.edu.cn (H.-Z. Chen).

0143-7208/$ - see front matter © 2006 Elsevier Ltd. All rights reserved.
doi:10.1016/j.dyepig.2006.08.035

were characterized by FTIR, element analysis, NMR, and UV–vis absorption. Some of their interesting aggregation behaviour and photoconductive properties resulting from the different length of the alkyl chain attached to perylene are also reported.

2. Experimental

2.1. Materials and equipments

Perylene-3,4,9,10-tetracarboxylic acid dianhydride (PTCDA), tetra-*n*-octylammonium bromide (TOAB), and alkyl halide (RBr) were purchased from Meryer Chemical Co. Polycarbonate (PC), and *N*,*N*′-diethyl-4-aminobenzaldehyde-1-phenyl-1′-α-naphthyl-hydrazone (BAH) were commercially available and used without further purification. All solvents used were of analytical grade and were distilled before use.

^{1}H NMR spectra were obtained on a Bruker Avance DMX500 nuclear resonance spectroscope. Elemental analyses data were determined on a Perkin–Elmer 240C elemental analyzer. The emission spectra were recorded on a Hitachi 4500 fluorescence spectrophotometer. UV–vis absorption spectra were taken on a Varian Cary 100 Bio spectrometer. The morphologies of the films were observed on a Skeio SPI3800N atomic force microscope (AFM). X-ray diffraction (XRD) measurements were performed at a Rigaku D/max-RA diffractometer with Cu Kα radiation. Optical texture pictures were taken on a Nikon Eclipse E600 microscope.

The films were prepared by casting solutions (0.01 M) of the PATC compounds in $CHCl_3$ onto either glass or quartz substrates and baking at 80 °C for 30 min to evaporate the solvent completely.

2.2. Synthesis

The synthetic route for the PTAC derivatives used in this work is shown in Scheme 1. Herewith a typical synthesis procedure for 3,4,9,10-tetra-(*n*-alkoxy-carbonyl)-perylene ($n = 4$, **Per4**): PTCDA (490 mg, 1.25 mmol) was converted to the tetrapotassium salt of the tetracarboxylic acid via stirring in aqueous potassium hydroxide solution (0.1 mol/L) at 70 °C. After filtration, the filtrate was acidified with aqueous hydrochloric acid solution (ca. 1 mol/L) until the pH was 8–9. To the ensuing dark red-green solution were added tetraoctyl ammonium bromide (TOAB) (0.2 g) and 1-bromobutane (10 mmol), and the mixture was refluxed under vigorous stirring. After 1–2 h, the solution became clear and colorless on top of which was a brown colored layer of oil. $CHCl_3$ was added to the mixture, and the $CHCl_3$ solution layer was collected and washed with 15% sodium chloride aqueous solution and deionized water. The resulting $CHCl_3$ solution was concentrated and precipitated by ethanol. The collected solid was washed with 100 mL ethanol three times and the product was dried under vacuum at 80 °C to give 0.75 g (yield 92%) of the product **Per4** as a golden yellow solid. ^{1}H NMR (500 MHz, $CDCl_3$), δ (ppm vs. TMS) = 1.01 (t, 12H), 1.51 (m, 8H), 1.80 (m, 8H), 4.33 (t, 8H), 7.93 (d, 4H), 8.08 (d, 4H). FTIR (KBr), $\nu = 2959.6$, 2871.9, 1724.5, 1589.1, 1277.4, 1171.8, 1135.0, 748.2 cm^{-1}. Anal. Calcd. for **Per4** ($C_{40}H_{44}O_8$): C, 73.60; H, 6.79%. Found: C, 73.30; H, 6.63%.

The remaining four PTAC derivatives (**Per6**, **Per8**, **Per10** and **Per12**) were prepared in a similar way. Their characterization is summarized below:

Per6: Yield 92%. ^{1}H NMR (500 MHz, $CDCl_3$), δ (ppm vs. TMS) = 0.91 (t, 12H), 1.81–1.35 (m, 32H), 4.33 (t, 8H), 7.92 (d, 4H), 8.08 (d, 4H). FTIR (KBr) $\nu = 2956.9$, 2929.1, 2861.2, 1725.8, 1719.6, 1698.2, 1587.7, 1469.8, 1276.0, 1167.6, 750.6 cm^{-1}. Anal. Calcd. for **Per6** ($C_{48}H_{60}O_8$): C, 75.36; H, 7.91%. Found: C, 75.10; H, 7.91%.

Per8: Yield 93%. ^{1}H NMR (500 MHz, $CDCl_3$), δ (ppm vs. TMS) = 0.89 (t, 12H), 1.29–1.84 (m, 48H), 4.33 (t, 8H), 7.93 (d, 4H), 8.08 (d, 4H). FTIR (KBr) $\nu = 2954.1$, 2926.3, 2852.8, 1731.8, 1713.5, 1274.5, 1165.0 cm^{-1}. Anal. Calcd. for **Per8** ($C_{56}H_{76}O_8$): C, 76.68; H, 8.73%. Found: C, 76.47; H, 8.72%.

Per10: Yield 94%. ^{1}H NMR (500 MHz, $CDCl_3$), δ (ppm vs. TMS) = 0.91 (t, 12H), 1.81–1.35 (m, 64H), 4.33 (t, 8H), 7.92 (d, 4H), 8.08 (d, 4H). FTIR (KBr) $\nu = 2956.3$, 2921.1, 2850.8, 1727.2, 1715.6, 1589.1, 1471.3, 1281.4, 1170.9, 1017.7, 747.1 cm^{-1}. Anal. Calcd. for **Per10** ($C_{64}H_{92}O_8$): C, 77.69; H, 9.17%. Found: C, 77.53; H, 9.40%.

Per12: Yield 93%. ^{1}H NMR (500 MHz, $CDCl_3$), δ (ppm vs. TMS) = 0.87 (t, 12H), 1.26–1.82 (m, 80H), 4.33 (t, 8H), 7.96 (d, 4H), 8.14 (d, 4H). FTIR (KBr) $\nu = 2953.3$, 2918.4, 2872.8, 2849.7, 1731.7, 1719.6, 1591.1, 1471.4, 1278.6, 1172.2, 1025.4, 747.1 cm^{-1}. Anal. Calcd. for **Per12** ($C_{72}H_{108}O_8$): C, 78.50; H, 9.88%. Found: C, 78.32; H, 10.30%.

2.3. Fabrication of photoreceptor and photoconductivity measurement

The photoconductivity of PTAC was studied in dual-layer photoreceptors that comprised a charge generation layer (CGL) and a charge transportation layer (CTL) on an aluminum substrate. The ~1 μm thick CGL was formed by casting the $CHCl_3$ solution containing 0.01 mol/L PTAC derivatives; the CTL consisted of 50 mass% BAH in PC matrix, of thickness 25 μm [13].

Photoconductivity measurements were carried out on a GDT-II model photoconductivity-measuring device by the standard photoinduced xerographic discharge technique [14]. The intensity of the exposure light (I) was 1.1 mJ^{-1} cm^2 during measurement using an incandescent lamp (5 W, 24 V) as light source. During measurement, the surface of the dual-layer photoreceptor was negatively charged in the dark. The photoinduced discharge curve was outputted by a computer, from which the residual potential (V_r) and time from original surface potential to half under illumination ($t_{1/2}$) were obtained. Photosensitivity was characterized by the half decay exposure energy ($E_{1/2}$), which is defined as the product of half decaying time ($t_{1/2}$) and the intensity of exposure light (I), i.e., $E_{1/2} = It_{1/2}$. A desired photoreceptor should have a large V_0 and a small V_r, and $t_{1/2}$. The smaller the $E_{1/2}$, the higher the photosensitivity of the photoreceptor[15].

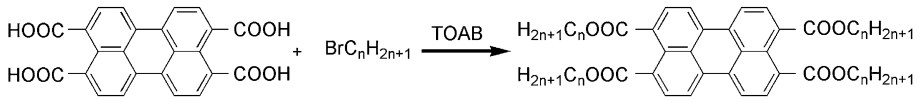

Per4: n=4 ; **Per6**: n=6 ; **Per8**: n=8 ; **Per10** n=10 ; **Per12**: n=12

Scheme 1. Synthetic route and chemical structures of PTAC derivatives used in this work.

3. Results and discussion

3.1. Synthesis

The synthetic route and the chemical structures of the five PTAC derivatives (**Per4**, **Per6**, **Per8**, **Per10**, and **Per12**) that were prepared using the PTC method are shown in Scheme 1; TOAB was used as the phase-transfer catalyst. The tetrapotassium salt of PTCDA was dissolved in the aqueous phase whose anions can then form cation–anion pairs by combination with the quaternary ammonium cations that are dissociated from TOAB. The hydrophobic cation–anion pairs tend to transfer to the organic phase of 1-bromoalkane, where the nuclear displacement reaction between perylene-3,4,9,10-tetracarboxylic anions and 1-bromoalkane (organic phase) takes place, giving the desired product, which precipitates in the aqueous phase during the reaction. The synthetic process is in agreement with the Starkes PTC model [16]. In this way, a small amount of organic soluble phase-transfer agent of TOAB can markedly increase the reaction rate and enable high yields (>90%) of satisfactory purity without further chromatographical purification.

Each of the five PTAC derivatives were readily soluble in common organic solvents and were carefully characterized by FTIR, ^{1}H NMR and elemental analysis; the results are consistent with the predicted chemical structures, demonstrating that the PTC method is indeed a simple and effective way to prepare PTAC derivatives.

3.2. Absorption and emission spectra

Solutions of all compounds in chloroform showed bright green-yellow fluorescence, even under daylight. No obvious difference was observed for the spectral properties in solution among these PTAC compounds indicating that the length of the alkyl chain does not affect their spectral properties in solution. Fig. 1(1) shows the typical absorption and fluorescence spectra of the PTAC derivatives (**Per8**) in diluted $CHCl_3$ solution. Both the absorption and fluorescence bands show a fine structure with two peaks and one shoulder. The absorption spectrum has a vibronic structure with two peaks at 444 and 472 nm and one shoulder at 417 nm, while the fluorescence peaks appear at 492 and 521 nm. Almost mirror symmetry between the absorption and the emission spectra is observed, although the relative intensity of the fluorescence peaks differs slightly from that of the absorption peaks. The absorption and fluorescence bands are reminiscent of those of pure perylene and correspond to S_0–S_1 transitions, the dipole moment of which is directed parallel to the long axis of the molecules [17,18]. Although the spectra of the PTAC derivatives are similar to that of the parent perylene compound (407, 436 nm), the observed red-shift (by 36 nm) in the band positions can be attributed to the four alkoxycarbonyl chains attached to perylene core.

No obvious distinction was found for their absorption in cast films (see Fig. 1(2)). The same three clearly resolved absorption bands as observed in solution remain for the PTAC compounds in the films although they become broader and red-shifted. With increasing alkyl chain length, the fine structure of the three absorption bands of the PTAC derivatives does not disappear, implying that no π–π interactions exist between adjacent PTAC molecules [19].

3.3. Aggregate structures

The crystallization behaviour of the PTAC derivatives films was examined by XRD measurements. As shown in Fig. 2, for the $n = 4$, 6, 8 homologues, the solid lattice constant was

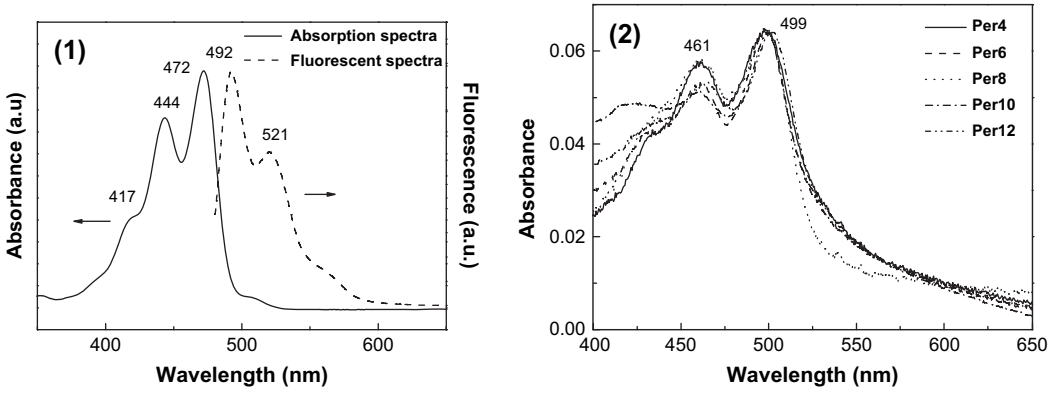

Fig. 1. (1) Representative normalized UV–vis absorption and luminescent spectra in $CHCl_3$ (**Per8**). (2) Normalized UV–vis absorption spectra of PTAC derivatives in casting films.

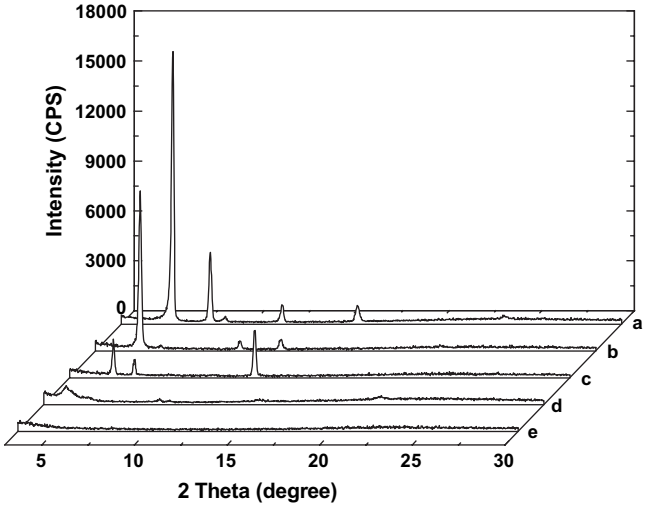

Fig. 2. X-ray diffraction patterns of PTAC derivatives in casting films (film thickness: about 500 nm): (a) **Per4**, (b) **Per6**, (c) **Per8**, (d) **Per10**, and (e) **Per12**.

similar to the column spacing, indicating the existence of a columnar structure. For comparison, the diffraction angle 2θ and the interplanar space d are summarized in Table 1. It is evident that the d value could be divided into two groups based on the diffraction peaks: the first group corresponds to the spacing between the columns and the second group corresponds to the intermolecular distance. For example, it was observed that in the first group, the ratios of all d values of **Per4** to 15.27 Å were exactly 1, 1/2, and 1/4, respectively; and in the second group the ratio of 5.62 to 11.32 Å was 1/2. The diffraction angle of 2θ became smaller with increasing alkyl chain length, indicating that the distance between the columns of PTAC derivatives increased in the film [20], so that a compact film could be obtained with a shorter alkyl chain. Meanwhile, the intensity of the diffraction peaks weakened with increasing length of the alkyl chains attached to perylene moiety. The diffraction peak was feeble for **Per10** ($n = 10$) and negligible for **Per12** with the longest alkyl chain ($n = 12$) in this study, implying low crystallinity for **Per10** and **Per12** [21].

The surface morphologies of the PTAC derivatives in cast films were observed using AFM (Fig. 3); large interconnected grains were observed for **Per4**, forming a continuous sheet film. Such kind of film is favorable in terms of charge transport, because efficient charge carrier transport through a semiconductor film requires that the film be continuous [16]. The continuous sheet film of **Per4** is thought to be related to its weak intermolecular repulsion arising from its short butyl chain. It can be seen that film morphology changed with increasing length of the alkyl chain. When the substituted alkyl chain is dodecyl, disconnected slices are observed in **Per10** film with some spherical particles in the slice. When the length of alkyl chain was dodecyl, continuous amorphous film (**Per12**) formed, as proven by XRD measurement. Such evolution of the film morphology suggests that the aggregate structure of the PTAC derivative films is affected significantly by the length of alkyl chain attached to the perylene core.

The evolution of the aggregation behaviour of the PTAC derivatives with increasing alkyl chain length was also studied using differential scanning calorimetry (DSC – Fig. 4). The PTAC derivatives investigated in this study have the typical molecular structure of discotic liquid crystal, namely a rigid aromatic core and several lateral flexible alkyl chains. As can be seen from Fig. 4, **Per4** exhibits a melting peak centered at 164.3 °C and a mesophase to isotropic peak centered at about 242.6 °C in the heating run of the DSC. **Per6** shows the melting transition at 85.7 °C and the isotropic phase transition at 187.3 °C in the heating run. The melting transition and the isotropic phase transition for **Per8** occurs at 63.8 and 137.1 °C, respectively. And, **Per10** and **Per12** with longer alkyl chain only have the melting point at 69.8 and 81.2 °C, respectively. The clear points decrease with increasing chain length from 242.6 °C ($n = 4$) to 137.1 °C ($n = 8$). The clear point cannot be found in DSC curves of **Per10** and **Per12**, implying the longest homologue with $n = 10$, 12 have no liquid crystalline phase.

However, when **Per10** film was slowly cooled down from the temperature of its isotropic state, liquid crystal texture was observed (see Fig. 5(d)). Fig. 5 shows the polarization microscope images of **Per4**, **Per6**, **Per8**, and **Per10** films which had been cooled down slowly from their isotropic phases. It is interesting that different textures are observed for these PTAC derivatives when cooled down slowly from the isotropic state to the mesomorphic temperature range, which is typical for columnar hexagonal liquid crystals [22]. All these observations suggest that **Per4**, **Per6**, **Per8**, and **Per10** possess the liquid crystalline phase with the exception of **Per12**, which does not exhibit the typical liquid crystal texture.

The liquid crystal character of PTAC derivatives, due to the aliphatic group attached to perylene core moiety, offers the chance of producing an ordered film. In order to see whether these ordered structures at liquid crystal phase could be kept in films at lower temperature, rapid cooling tests were carried out. As shown in Fig. 6, distinct differences were observed for the PTAC derivatives. **Per4** film was broken during rapid cooling due to the molecular rigidity resulting from the shorter alkyl chain. When the substituted alkyl was replaced

Table 1
The diffraction angle 2θ and the interplanar space d for PTAC derivatives

Samples	2θ and d				
Per4	5.78°, 15.27 Å	11.66°, 7.58 Å	23.66°, 3.76 Å	7.80°, 11.32 Å	15.74°, 5.62 Å
Per6	5.42°, 16.29 Å	10.80°, 8.18 Å	–	6.51°, 13.56 Å	13.04°, 6.78 Å
Per8	5.36°, 16.47 Å	–	–	6.52°, 13.54 Å	13.00°, 6.80 Å
Per10	4.22°, 20.91 Å	–	–	–	–

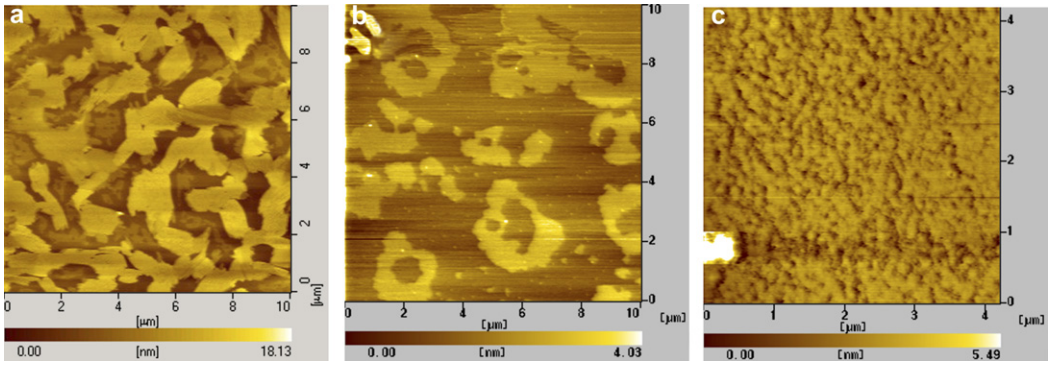

Fig. 3. AFM images of PTAC derivatives in casting films on mica substrates: (a) **Per4**, (b) **Per10**, and (c) **Per12**.

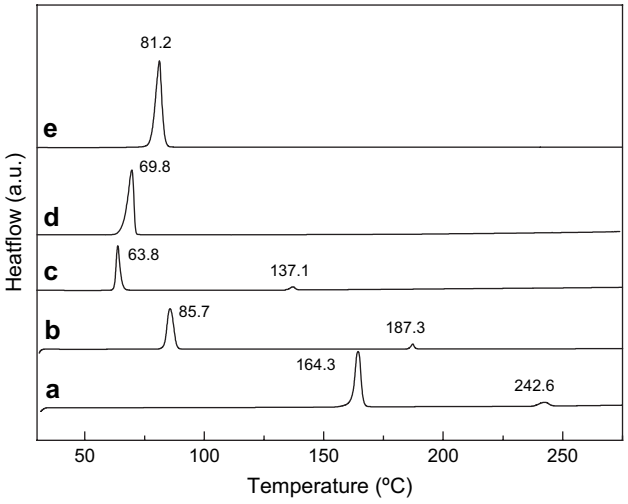

Fig. 4. DSC curves of PTAC derivatives: (a) **Per4**, (b) **Per6**, (c) **Per8**, (d) **Per10**, and (e) **Per12**. Scan rate is 10 °C/min.

by the longer hexyl or octyl groups, no obvious difference was observed in film morphology during rapid cooling under cross-polarizer microscope due to the better flexibility of these longer (hexyl and octyl) chains. **Per10**, however, could not hold the ordered structure during rapid cooling due to its narrow liquid crystal range.

3.4. Photoconductivity

In order to study the influences of molecular structures and aggregate behaviors on the photoconductivity of PTAC compounds, we fabricated dual-layered photoreceptors. The change in the photosensitivity (S) and residual potential (V_r) of PTAC with different alkyl chains is given in Table 2. We can find that, under the same exposure conditions and with the same CTL, the photoreceptor from **Per12** shows a photosensitivity of 2.02 $mJ^{-1}\,cm^2$. After decreasing the length of alkyl chain slightly to decanyl (**Per10**), the photosensitivity increases slightly to 2.93 $mJ^{-1}\,cm^2$. The photosensitivity further

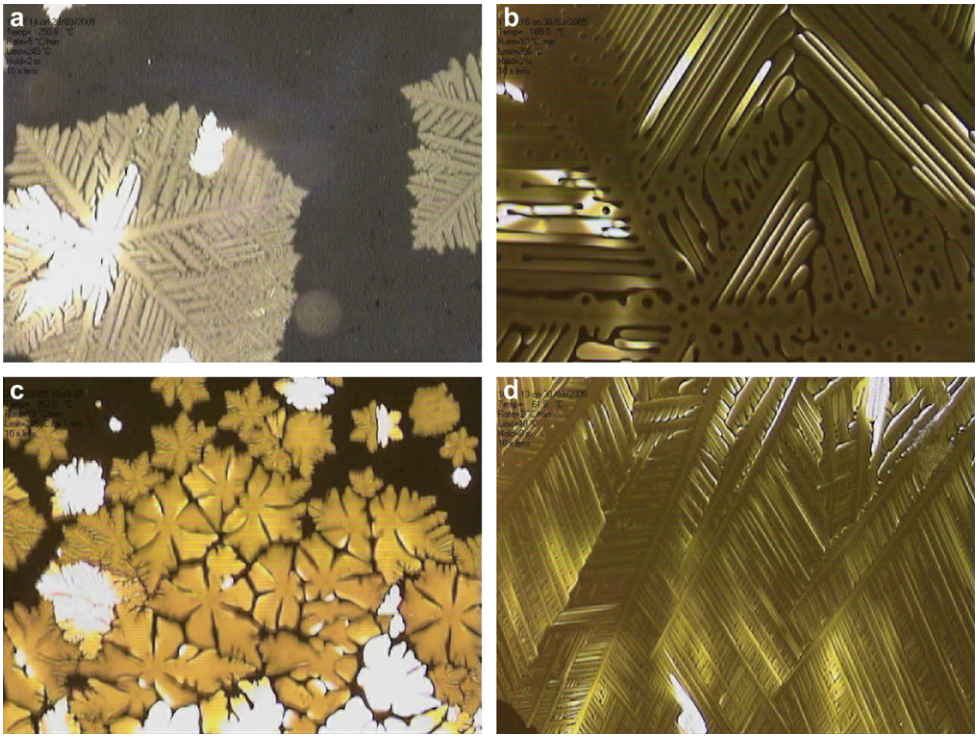

Fig. 5. Optical textures of (a) **Per4**, (b) **Per6**, (c) **Per8**, and (d) **Per10** films cooled down slowly from the isotropic phase (magnified 100×).

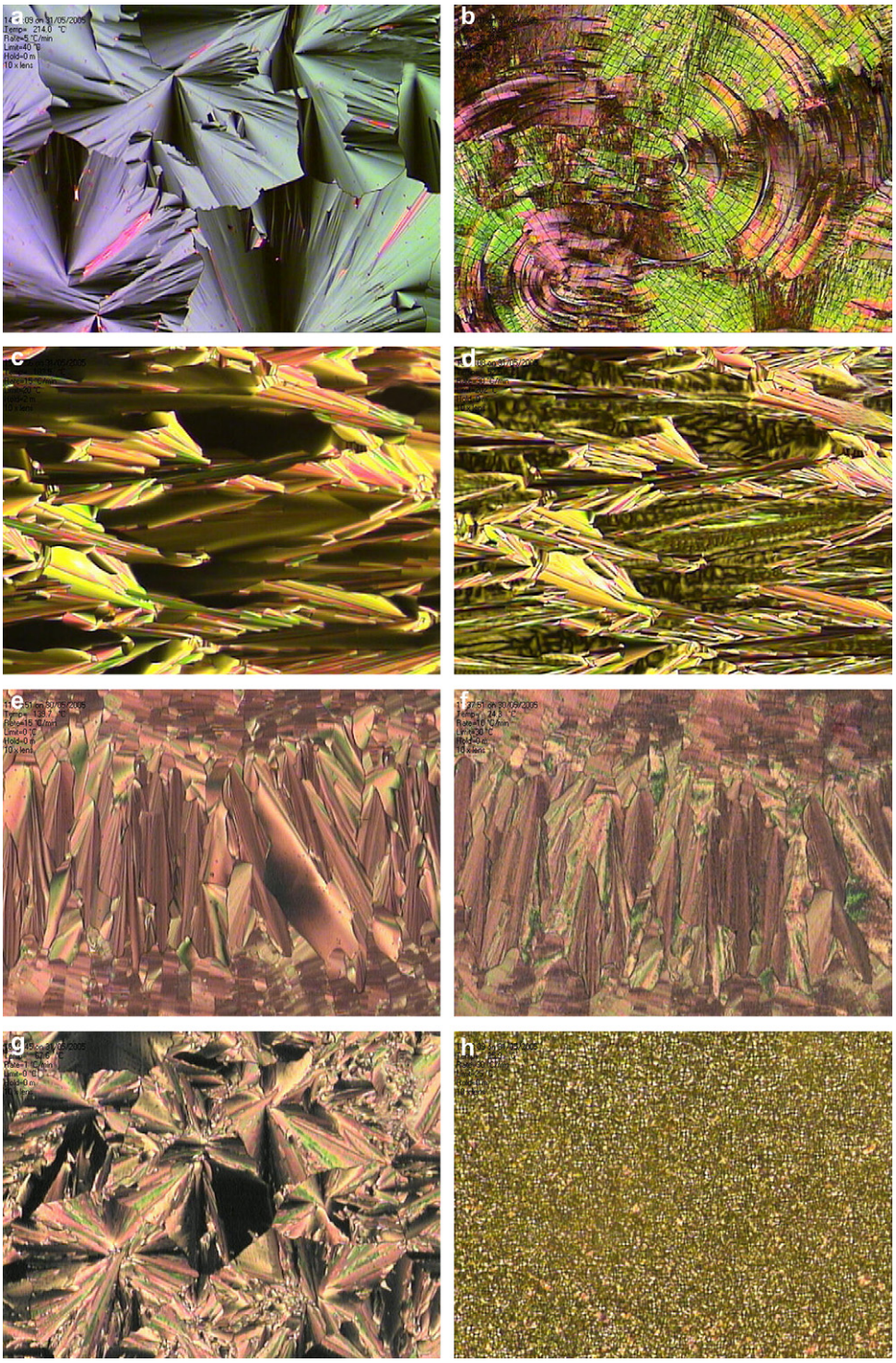

Fig. 6. Optical textures of **Per4** film under cross-polarizer at 214 °C (a) and being cooled down rapidly to 27 °C (b); **Per6** film at 183 °C (c) and being cooled down rapidly to 52 °C (d); **Per8** film at 140 °C (e) and being cooled down rapidly to 25 °C (f); **Per10** film at 68 °C (g) and being cooled down rapidly to 26 °C (h). The cooling rate for all samples is 100 °C/min.

increases with decreasing length of the alkyl chain, and reaches the highest of 90.91 mJ^{-1} cm^2 for **Per4**, 45-fold higher than that of **Per12**. It is also found that residual potential (V_r) of these photoreceptors decreases gradually with decreasing alkyl chain length attached to perylene moiety, and reaches the lowest for **Per4**, indicating that the photoconductivity increases with decreasing length of attached alkyl chain for PTAC derivatives as well. The significant change of photosensitivity for PTAC derivatives used in this study is thought to be related with their morphologies in film because they own the same photoactive perylene core. As demonstrated from XRD and AFM results earlier, the PTAC derivatives tend to form

Table 2
Photosensitive parameters of PTAC derivatives

	V_r (V)	$t_{1/2}$(s)	S (mJ^{-1} cm^2)[a]
Per4	46	0.01	90.91
Per6	112	0.08	11.36
Per8	171	0.19	4.78
Per10	213	0.31	2.93
Per12	281	0.45	2.02

[a] The photosensitivity $S = E_{1/2}^{-1}$ (mJ^{-1} cm^2), being exposed to white light of 1.1 mJ^{-1} cm^2. Initial surface potential is about 850 V.

a crystal film by decreasing the length of the attached alkyl chain. **Per4** can form continuous and ordered crystal film while **Per12** forms amorphous film by solution-casting method. The continuous and ordered crystal film endows better charge transportation than the amorphous film does, leading to higher photosensitivity for **Per4** when compared to **Per12**. XRD results also suggest that the more ordered and crystalline film forms with decreasing length of the alkyl chain, indicating that the longer chain prevents molecules from packing tightly and orderly to form crystal form, leading to worse photosensitivity for longer chains.

4. Conclusions

In summary, a series of PTAC derivatives of satisfactory purity and high yield were obtained via a phase-transfer catalysis method in a single-step by using readily available starting materials under mild conditions, which provides a simple approach to synthesize soluble PTAC derivatives as well as other complicated organic semiconductors. The length of the alkyl chains attached to the perylene skeleton had a great effect on aggregation in films, which was interpreted in terms of different aggregate structures. Photosensitivity increased with decreasing length of alkyl attached to perylene and reached a maximum for **Per4**, this being some 45 times higher than that of **Per12** when exposed to white light. The more ordered and crystalline film could be formed with decreasing length of alkyl chain attached to perylene core, which is favorable for charge transport. The results offer help in the design of high-performance photoconductive materials.

Acknowledgements

This work was supported by the National Natural Science Foundation of China (Nos. 50225312, 50433020, 50403022, 50520150165).

References

[1] Tang CW. Two-layer organic photovoltaic cell. Applied Physics Letters 1986;48:183–5.
[2] Yakimov A, Forrest SR. High photovoltage multiple-heterojunction organic solar cells incorporating interfacial metallic nanoclusters. Applied Physics Letters 2002;80:1667–9.
[3] Peumans P, Uchida S, Forrest SR. Efficient bulk heterojunction photovoltaic cells using small-molecular-weight organic thin films. Nature 2003;425:158–62.
[4] Schmidt-Mende L, Fechtenkötter A, Müllen K, Moons E, Friend RH, MacKenzie JD. Self-organized discotic liquid crystals for high-efficiency organic photovoltaics. Science 2001;293:1119–22.
[5] Horowitz G, Kouki F, Spearman P, Fichou D, Nogues C, Pan X, et al. Evidence for n-type conduction in a perylene tetracarboxylic diimide derivative. Advanced Materials 1996;8:242–5.
[6] Malenfant PRL, Dimitrakopoulos CD, Gelorme JD, Kosbar LL, Graham TO, Curioni A, et al. n-Type organic thin-film transistor with high field-effect mobility based on a *N*,*N*′-dialkyl-3,4,9,10-perylene tetracarboxylic diimide derivative. Applied Physics Letters 2002;80:2517–9.
[7] Ranke P, Bleyl I, Simmerer J, Haarer D, Bacher A, Schmidt HW. Electroluminescence and electron transport in a perylene dye. Applied Physics Letters 1997;71:1332–4.
[8] Kalinowski J, Macro PD, Cocchi M, Fattori V, Camaioni N, Duff J. Voltage-tunable-color multilayer organic light emitting diode. Applied Physics Letters 1996;68:2317–9.
[9] Biadasz A, Hertmanowski R, Martynski T, Inglot K, Bauman D. Langmuir films of dichroic dyes with fluorescent properties. Dyes and Pigments 2003;56:209–17.
[10] Stolarski R, Fiksinski KJ. Fluorescent perylene dyes for liquid crystal displays. Dyes and Pigments 1994;24:295–303.
[11] Hassheider T, Benning SA, Kitzerow HS, Achard MF, Bock H. Color-tuned electroluminescence from columnar liquid crystalline alkyl arenecarboxylates. Angewandte Chemie International Edition 2001;40:2060–3.
[12] Qin YJ, Shi JH, Wu W, Li XL, Guo ZX, Zhu DB. Concise route to functionalized carbon nanotubes. Journal of Physical Chemistry B 2003;107:12899–901.
[13] Cao L, Chen HZ, Wang M, Sun JZ. Photoconductivity study of modified carbon nanotube/oxotitanium phthalocyanine composites. Journal of Physical Chemistry B 2002;106:8971–5.
[14] Shi MM, Chen HZ, Wang M, Ye J. Photoconductivity of fluoroperylene diimide/PVK composite. Synthetic Metals 2003;137:1537–8.
[15] Charles MS. Phase-transfer catalysis. I. Heterogeneous reactions involving anion transfer by quaternary ammonium and phosphonium salts. Journal of the American Chemical Society 1971;93:195–9.
[16] Greeg BA, Cormier RA. Liquid crystal perylene diimide films characterized by electrochemical, spectroelectrochemical, and conductivity versus potential measurements. Journal of Physical Chemistry B 1998;102:9952–7.
[17] Hertmanowski R, Biadasz A, Martyński T, Bauman D. Optical spectroscopy study of some 3,4,9,10-tetra-(*n*-alkoxy-carbonyl)-perylenes in Langmuir–Blodgett films. Journal of Molecular Structure 2003;646:25–33.
[18] Newman CR, Frisbie CD, da Silva Filho DA, Bredas JL, Ewbank PC, Mann KR. Introduction to organic thin film transistors and design of *n*-channel organic semiconductors. Chemistry of Materials 2004;16:4436–51.
[19] Graser F, Hädicke E. Crystal structure and color of perylene-3,4,9,10-bis(dicarboximide) pigments. Liebigs Annalen der Chemie 1980;1994–2011.
[20] Mo X, Chen HZ, Wang Y, Shi MM, Wang M. Fabrication and photoconductivity study of copper phthalocyanine/perylene composite with bulk heterojunctions obtained by solution blending. Journal of Physical Chemistry B 2005;109:7659–63.
[21] Shi MM, Chen HZ, Shi YW, Sun JZ, Wang M. Unique aggregate structure of fluoroperylene diimide thin film. Journal of Physical Chemistry B 2004;108:5901–4.
[22] Benning S, Kitzerow HS, Bock H, Achard MF. Fluorescent columnar liquid crystalline 3,4,9,10-tetra-(*n*-alkoxycarbonyl)-perylenes. Liquid Crystals 2000;27:901–6.